Mass spectroscopic study for vaporization characteristics of $Ba(TMHD)_2$ and $Sr(TMHD)_2$ in electron cyclotron resonance-plasma enhanced metal organic chemical vapor deposition

Joon Sung Lee, Han Wook Song, Kyong Sub Kim, Byoung Gon Yu,[a] Yon Ho Jeong,[b] Zhong-Tao Jiang, and Kwangsoo No[c]
Department of Materials Science and Engineering, Korea Advanced Institute of Science and Technology, Taejon, Korea

(Received 23 February 1996; accepted 6 September 1996)

The decomposition and the degradation characteristics of $Ba(TMHD)_2$ and $Sr(TMHD)_2$ with storage time were analyzed using differential scanning calorimetry. Mass spectrometer monitoring of source vapors with Ar and NH_3 carrier gases in an electron cyclotron resonance-plasma enhanced metal organic chemical vapor deposition system was also performed. Introducing NH_3 as a carrier gas, significantly improved the volatility and the thermal stability of the precursors, as well as the uniformity and the surface smoothness of strontium carbonate films. Required vaporization temperatures of the precursors were lower with the introduction of NH_3 gas than with conventional Ar carrier gas. The degradation with the storage time and with oligmerization at the evaporation temperature for $Ba(TMHD)_2$ was greater compared to $Sr(TMHD)_2$. © *1997 American Vacuum Society*. [S0734-2101(97)00101-2]

I. INTRODUCTION

High dielectric materials are the most promising capacitor materials for giga bit scale dynamic random access memories (DRAMs) designed with a simple cell structure. Among numerous high dielectric materials, paraelectric $SrTiO_3$ and $(BaSr)TiO_3$ are attractive because of their high dielectric constant, good thermal stability, and good high frequency characteristics.

Several deposition techniques, such as rf-sputtering,[1–3] reactive coevaporation,[4] and metal organic chemical vapor deposition (MOCVD)[5–10] have been reported for $SrTiO_3$ and $(BaSr)TiO_3$ films. Among these techniques, MOCVD is often considered to be the best for its high deposition rate, easy composition control, easy scale up to manufacturing volumes, and excellent coverage of surface irregularities for high density DRAM application. However, the MOCVD technique is highly dependent on the availability of MO-sources.

A primary consideration is that the MO-sources should vaporize to provide appropriate metal chelate vapor concentration at fixed evaporation temperature chosen to form in the desired compositions of the mixed oxide films, such as, $SrTiO_3$ and $(BaSr)TiO_3$. The 2,2,6,6,-tetramethyl-3,5-heptanedione (TMHD) compounds of Ba and Sr were selected as the MO-sources because of their low toxicity and carbon, and lack of fluorine contamination in films. However, they have three major problems.[11] The first is that $Ba(TMHD)_2$ and $Sr(TMHD)_2$ degrade with time, even at room temperature, which brings poor reproducibility. The second is that they have low vapor pressures, even at relatively high evaporation temperature, resulting in a low deposition rate of oxide films. (In order to solve this, a special evaporator system is needed.) The third is that they partially decompose and become nonvolatile chemical species during the evaporation process, which causes their vapor phase concentrations to drop as a function of deposition time at fixed evaporation temperatures.

In this study, MO-sources have been characterized by differential scanning calorimetry (DSC). Their vapors in the deposition chamber have been analyzed by mass spectrometry/residual gas analysis (RGA). A membrane evaporator has been used to increase the vapor pressure of the MO-sources, and an ECR plasma has been employed to increase the activation and the decomposition of these vapors in the deposition chamber. We also used NH_3 as a carrier gas to stabilize and enhance the vaporization rate of the sources. In this sense, the effects of NH_3 carrier gas on the transport and the decomposition characteristics of MO-sources with time were investigated by *in situ* monitoring with mass spectrometry/RGA in the electron cyclotron resonance-plasma enhanced metal organic chemical vapor deposition (ECR-PEMOCVD) system. Strontium carbonate films were prepared by an ECR-PEMOCVD process using Ar or NH_3 as a carrier gas. The films were characterized by ellipsometry, a color chart, scanning electron microscopy (SEM), and x-ray diffraction (XRD).

II. EXPERIMENT

We conducted thermal analysis on $Ba(TMHD)_2$ and $Sr(TMHD)_2$ with time using DSC (Mac. Science DSC-3110) in 200 sccm nitrogen. The MO-sources were heated up to 300 °C and cooled down to room temperature at a rate of ± 10 °C min.

The transport and the decomposition characteristics of MO-source vapors were *in situ* monitored in an ECR-

[a]Electronics and Telecommunications Research Institute, Taejon, Korea.
[b]Mando Machinery Corporation Research and Development Center, Kyongki-Do, Korea.
[c]Electronic mail: ksno@cais.kaist.ac.kr

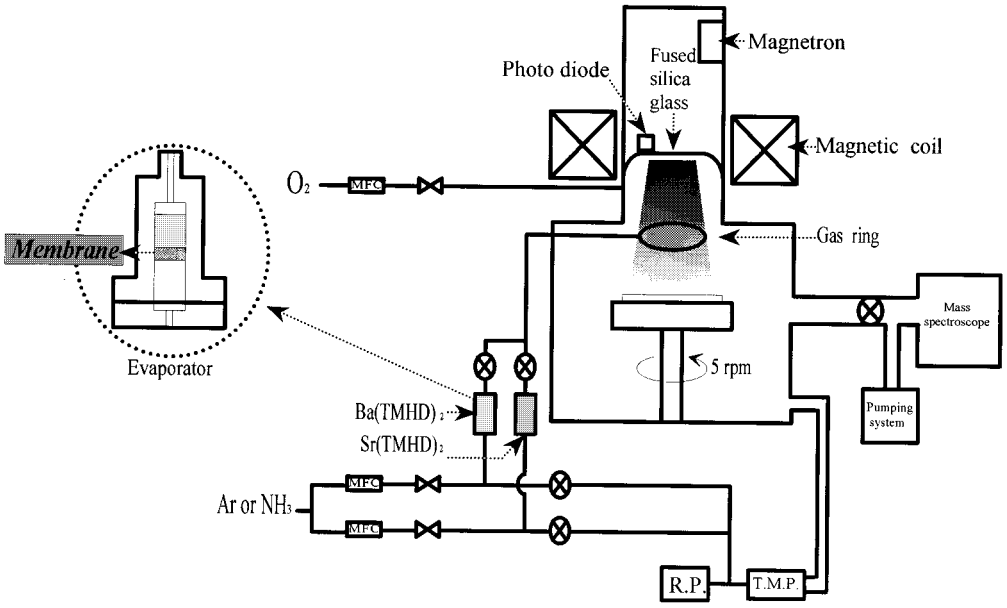

FIG. 1. A schematic diagram of the ECR-PEMOCVD system adapted to a mass spectrometry/RGA system.

PEMOCVD system (Kim's Vacuum Co. Ltd) using a mass spectrometry/RGA (VG Instruments, micromass 200 F). A schematic diagram of the ECR-PEMOCVD with a mass spectrometry/RGA system is shown in Fig. 1. The microwave plasma power, the pressure of the deposition chamber, and the pressure of the mass spectrometry/RGA were fixed at 200 W, 3×10^{-3} Torr, and 2×10^{-5} Torr, respectively. $Ba(TMHD)_2$ and $Sr(TMHD)_2$ were used as the metal organic sources, oxygen was used as the oxidant, and the Ar or NH_3 was used as the carrier gas. The flow rate of carrier gas (Ar or NH_3) was kept at 15 sccm during the experiment. In order to increase the vapor pressure of the MO-sources [$Ba(TMHD)_2$ and $Sr(TMHD)_2$] by increasing the contact surface area, membrane evaporators were incorporated and heated by heating tapes. The stainless steel membranes consists of 5 μm pores, so that the Ar or NH_3 carrier gas can go through them. This modification significantly increased the deposition rate of films. The gas lines from the evaporators to the gas ring in the reaction chamber were heated as well to prevent condensation of the source vapors. Oxygen introduced into the plasma generation chamber to generate plasma was also heated to reduce the chance of condensation due to cold gas incorporation. The substrate used here was a Si(p-type 100) wafer, which was rotated at 5 rpm and heated by a resistance heater during the deposition. The pumping system consisted of a series; a turbomolecular pump (TMP) and a rotary pump (RP). The pressure in the reaction chamber was controlled by a conductance controllable valve, and the plasma matching was adjusted by a photo-diode.

The thickness of strontium carbonate films was measured by an ellipsometry and cross-sectional SEM. The films were characterized by SEM and XRD.

III. RESULTS AND DISCUSSION

A. Thermal analysis

Figure 2 shows DSC data from as-received $Ba(TMHD)_2$ and after three months storage. The DSC data of as-received precursor [Fig. 2(a)] shows two endothermic peaks at 150.9 and 190.6 °C upon heating, but no peak during the cooling. Both peaks represent the melting of $Ba(TMHD)_2$.[12] Figure 2(b) shows DSC data of $Ba(TMHD)_2$ powder stored for three months in a packed state in a dry box after received. There are many unknown endothermic and exothermic peaks.

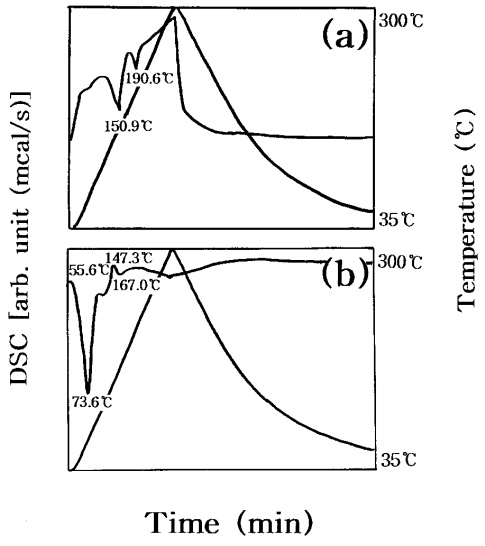

FIG. 2. DSC data of $Ba(TMHD)_2$: (a) as-received and (b) stored for three months.

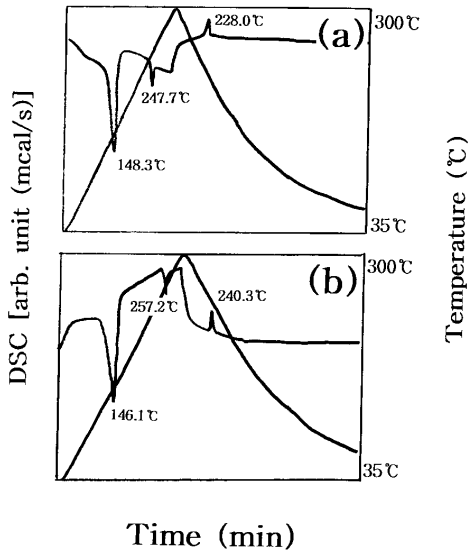

FIG. 3. DSC data of $Sr(TMHD)_2$: (a) as-received and (b) stored for three months.

These observations infer that $Ba(TMHD)_2$ was drastically degradated with time and changed to absolutely different chemical species even at room temperature. The powder color changed from white for as-received to yellow after three months of storage.

Figure 3 shows DSC data of as-received $Sr(TMHD)_2$ and after three months storage. The DSC data of as-received precursor [Fig. 3(a)] shows endothermic peak at 148.7 °C and a sharp endothermic peak at 247.7 °C upon heating, and a sharp exothermic peak at 228 °C during the cooling. Both peaks observed upon heating represent the melting of $Sr(TMHD)_2$, and the peak observed during the cooling represents the solidification. Fig. 3(b) shows the DSC data of $Sr(TMHD)_2$ stored for three months in a packed state in a dry box after received. The second and third peaks shift to higher temperatures compared to Fig. 3(a). These observations infer that $Sr(TMHD)_2$ was degradated with time and changed to a different chemical species even at room temperature. The powder color changed from light yellow for as-received to dark yellow after three months storage. Based on Figs. 2 and 3, we can conclude that the $Ba(TMHD)_2$ and $Sr(TMHD)_2$ degradated with time even at room temperature, and moreover, the $Ba(TMHD)_2$ degradates more seriously than $Sr(TMHD)_2$ under the same condition. A possible cause of the observed difference in degradation rates between the two precursors could be the difference in the radius of the metal ions. Generally, the β-diketonate complexes are coordinatively unsaturated and are therefore prone to be oligomerized and/or coordinated by solvent molecules, especially water. The degree of the coordinatively unsaturization increases as the radius of the metal ion increases. This degradation problem of MO-sources has been known to bring weak reproducibility of MOCVD processed $SrTiO_3$ and $(BaSr)TiO_3$ films.

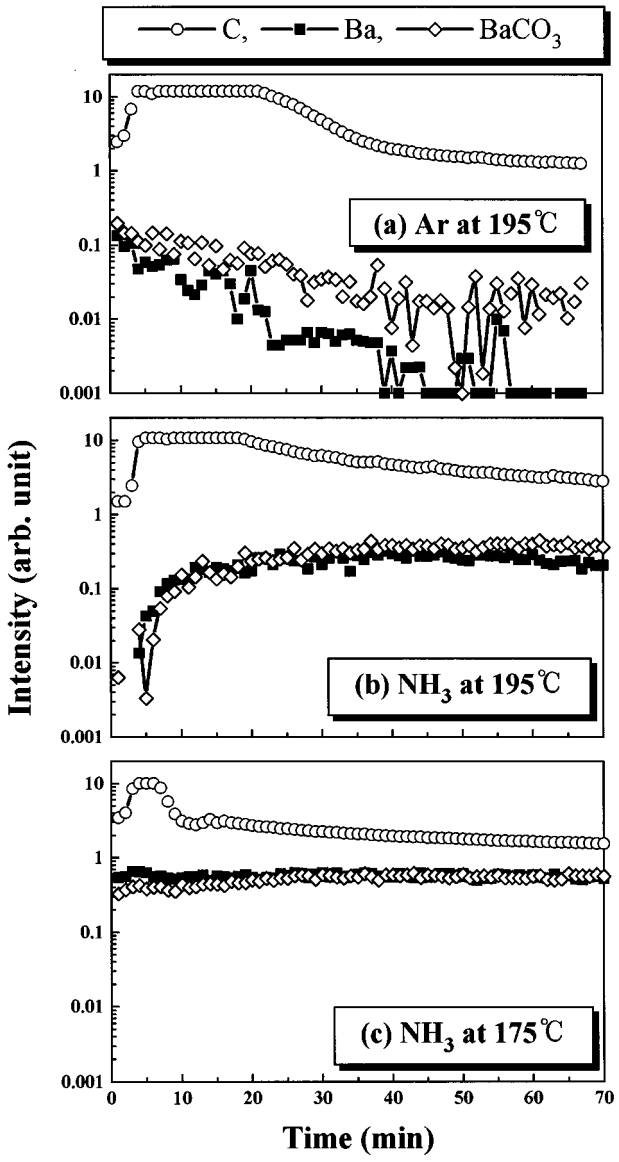

FIG. 4. Plots of the signal intensity vs time of various vapor species in mass spectra of the $Ba(TMHD)_2$ precursor evaporated with different carrier gases and at different temperatures: (a) with Ar at 195 °C, (b) with NH_3 at 195 °C, and (c) with NH_3 at 175 °C.

B. *In situ* mass spectra

To obtain stoichiometric and compositional uniformity in the deposited films, the vapor pressures of each precursor must be held constant during the deposition process. Therefore, we investigated the vaporization characteristics of MO-source pressures using mass spectrometer/RGA. The vapors from the heated MO-source were transported by Ar (or NH_3) gas to the deposition chamber. The temperatures of the MO-sources were raised from room temperature to ~175–195 °C for the $Ba(TMHD)_2$ and to ~205–225 °C for the $Sr(TMHD)_2$, and then maintained for about 6–8 min.

Figure 4 includes the plots of the signal intensity versus time for various vapor species in the mass spectra of as-received $Ba(TMHD)_2$ precursors evaporated with different

carrier gases and at different temperatures. Figure 4(a) shows the plot of the precursor evaporated with Ar carrier gas at 195 °C. The evaporation temperature was chosen based on the DSC data [Fig. 2(a)]. The intensity of the species of carbon, to which the mass corresponds, drastically increased in the initial period of the evaporation and then decreased as the evaporation proceeded. (The constant region between them was due to the upper limitation of the instrument.) The initial increase was due to the time required to heat the evaporator. The intensities of the species to which the masses correspond, Ba and $BaCO_3$, continuously decreased during the whole evaporation process. Because of noise the spectra for Ba and $BaCO_3$ appeared unstable in the relatively low intensity region. These observations may indicate that a certain amount of the vapor containing Ba evaporates in the initial part of the evaporation but gradually decreases due to the gradual degradation of $Ba(TMHD)_2$ as the evaporation proceeds. Figures 4(b) and 4(c) show the plots of signal intensity versus time of various vapor species in the mass spectra of the $Ba(TMHD)_2$ precursor evaporated with NH_3 carrier gas at 195 and 175 °C, respectively. In Fig. 4(b), the intensity of carbon, the species to which the mass corresponds, drastically increases in the initial period of the evaporation and then decreases as the evaporation proceeds. Compared with Ar [Fig. 4(a)], NH_3 carrier gas increases the carbon vapor pressure and makes it more stable at the same temperature; e.g., 195 °C in Fig. 4(b). The intensities of the species with masses corresponding to Ba and $BaCO_3$ rapidly increase during the initial part of the evaporation and then keep almost constant levels during the process. The initial increment of evaporation is due to the time required to heat up the precursor. These observations may indicate that the gradual degradation of $Ba(TMHD)_2$ is not affected significantly by the NH_3 carrier gas during the evaporation process, so that a thin film having relatively high compositional uniformity could be obtained by using this method. The plot in Fig. 4(c) has a similar shape to that shown in Fig. 4(b), indicating no gradual degradation with NH_3 carrier gas. The intensities of the species with masses corresponding to Ba and $BaCO_3$ are higher at the evaporation temperature of 175 °C [0.4–0.6 in Fig. 4(c)] than at 195 °C [0.2–0.4 in Fig. 4(b)], which indicates that the higher vapor pressure of Ba may be obtained using NH_3 carrier gas at a lower temperature of 175 °C. A similar study has been carried out for the as-received $Sr(TMHD)_2$ precursor. Figure 5(a) shows the plot of the precursor evaporated with Ar carrier gas at 225 °C. The evaporation temperature was chosen based on the DSC data [Fig. 3(a)]. The intensity of the species with mass corresponding to carbon drastically increased in the initial period of the evaporation and then decreased as the evaporation proceeded. The intensity of the species whose mass corresponds to $SrCO_3$ continuously decreased during the whole evaporation process. The species with mass corresponding to Sr was not detected. These observations may indicate that Sr evaporates during the initial part of the evaporation process, and decreases as $Sr(TMHD)_2$ degrades as the evaporation proceeds. Figures 5(b) and 5(c) show the plots of signal intensity versus time of various vapor species in the mass spectra of the $Sr(TMHD)_2$ precursor evaporated with NH_3 carrier gas at 225 °C and 205 °C, respectively. In Fig. 5(b), the intensity of the species with mass corresponding to carbon drastically increases in the initial period of the evaporation and decreases as the evaporation proceeds. The intensity of the species with mass corresponding to Sr dramatically changes and decreases as the evaporation proceeds, but the species with mass corresponding to $SrCO_3$ is constant during the entire evaporation process except at the onset. In Fig. 5(c), the intensity of the species with mass corresponding to carbon remains almost a constant value during the whole evaporation process except the initial part which is due to the heating time of the evaporator. The intensities of the species whose

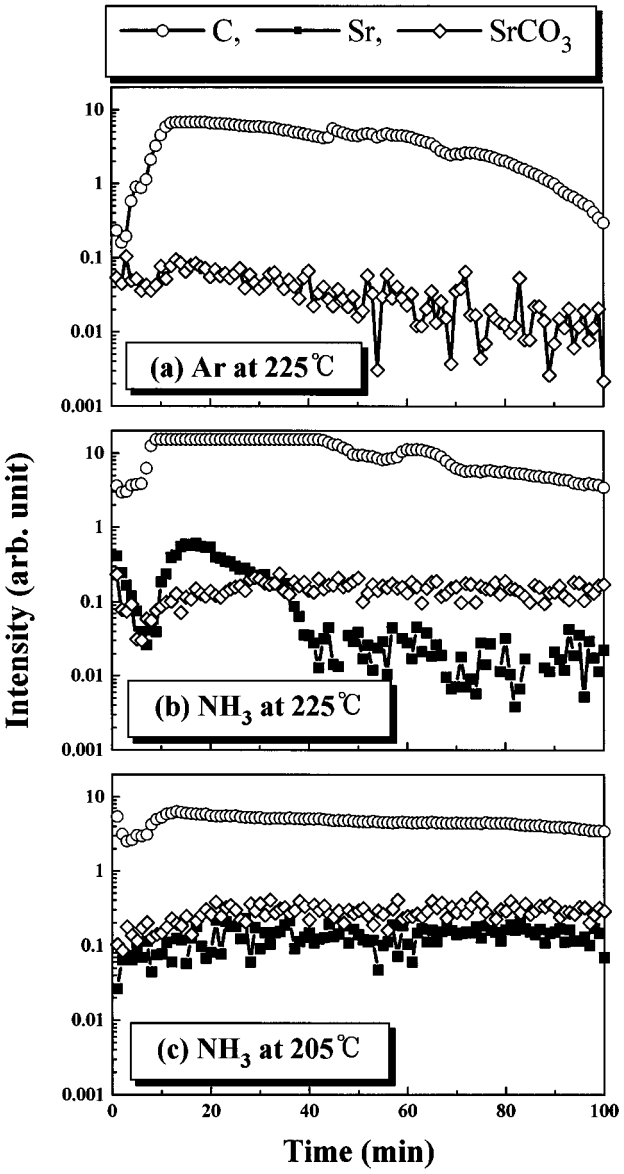

FIG. 5. Plots of the signal intensity vs time of various vapor species in mass spectra of the $Sr(TMHD)_2$ precursor evaporated with different carrier gases and at different temperatures: (a) with Ar at 225 °C, (b) with NH_3 at 225 °C, and (c) with NH_3 at 205 °C.

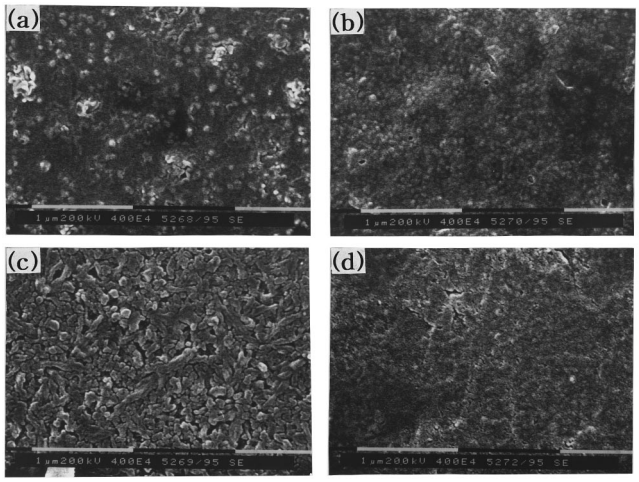

FIG. 6. Scanning electron micrographs of films deposited with different carriers gases and at different evaporation temperatures: (a) with Ar at 210 °C, (b) with NH_3 at 210 °C, (c) with Ar at 200 °C, and (d) with NH_3 at 180 °C.

masses correspond to Sr and $SrCO_3$ also remain at constant values, except at the initial stage, and are higher (~0.3) than those observed in the case of the evaporation temperature of 225 °C (0.1–0.2). These observations indicate that the precursor evaporation temperature can be reduced from 225 to 205 °C for obtaining higher Sr vapor pressure, as well as uniformity, using NH_3 instead of Ar as a carrier gas.

C. Microstructures

To compare the microstructures of films deposited with different carrier gases, but similar in thickness, we deposited the films for a short time (20 min) at different evaporation temperatures (160–225 °C) using $Sr(TMHD)_2$. The thickness difference between the films fabricated using NH_3 (or Ar) as a carrier gas increased with deposition time, or as evaporation temperatures decreased. This was due to the degradation of the MO precursor as we described in the previous sections. Figure 6 shows microstructures of films, which have similar thicknesses (1200–1400 Å), deposited with different carrier gases at different evaporation temperatures. The substrate temperature was 400 °C for all the films fabricated. Figures 6(a) and 6(b) are the SEM microstructures of the films deposited with Ar and NH_3 carrier gases, respectively, but at the same evaporation temperature of 210 °C. The film deposited with Ar carrier gas [Fig. 6(a)] has rough and nonuniform microstructure, but that deposited with NH_3 carrier gas [Fig. 6(b)] has smooth and uniform microstructure. Figure 6(c) shows the microstructure of the film deposited with Ar carrier gas at 200 °C which has a porous and large grain structure and Fig. 6(d) shows the microstructure of the film deposited with NH_3 carrier gas at 180 °C which has a dense and fine grain structure. We also found that the evaporation temperature, as well as the type of carrier gas, affects the microstructure by comparing Figs. 6(b) and 6(d).

IV. CONCLUSION

The decomposition and degradation characteristics of $Ba(TMHD)_2$ and $Sr(TMHD)_2$ with time were analyzed using DSC. Both $Ba(TMHD)_2$ and $Sr(TMHD)_2$ degradate with time even at room temperature, and moreover, the $Ba(TMHD)_2$ degradates more seriously than $Sr(TMHD)_2$ at the same condition. A possible cause of the observed difference in degradation rates between the two precursors may be due to the different radii of metal ions. The mass spectra *in situ* monitored from the vapors of $Ba(TMHD)_2$ and $Sr(TMHD)_2$ using Ar and NH_3 carrier gases in a ECR-PEMOCVD system were also obtained. The degree of degradation of $Ba(TMHD)_2$ is greater than that of $Sr(TMHD)_2$ during the evaporation process. It has been found that using NH_3 carrier gas for the β-diketonate ligand greatly increases the vaporization rate of these alkaline earth-metal chelates and restricts the degradation of MO-sources, probably owing to adduct formation accompanying the dissociation of the oligomers. The required MO-source temperatures using NH_3 as a carrier gas are lower than those using conventional Ar carrier gas. However, it is found that NH_3 is insufficient to restrict degradation at relatively high evaporation temperatures. All films deposited with NH_3 carrier gas have smoother and denser microstructures than those deposited with Ar carrier gas. The difference between the microstructures can be explained by different decomposition or degradation characteristics of MO-sources. The microstructure of the films was also affected by evaporation temperature of the MO-source and carrier gas. In the view of preparation of $SrTiO_3$ or $(BaSr)TiO_3$ films, NH_3 gas makes it possible to stabilize composition of films in thickness, increase the deposition rate, and obtain uniform and dense microstructures.

ACKNOWLEDGMENTS

This work was supported by the Electronics and Telecommunications Research Institute and the Ministry of Science and Technology, Korea.

[1]W. B. Pennebaker, IBM J. Res. Develop. 686 (1969).
[2]S. Matsubara, T. Sakuma, S. Yamamichi, H. Yamaguchi, and Y. Miyasaka, Mater. Res. Soc. Symp. Proc. **200**, 243 (1990).
[3]T. Sakuma, S. Yamamichi, S. Matsubara, H. Yamaguchi, and Y. Miyasaka, Appl. Phys. Lett. **57**, 2431 (1990).
[4]H. Yamaguchi, S. Matsubara, and Y. Miyasaka, Jpn. J. Appl. Phys. **30**, 2197 (1991).
[5]H. Yamaguchi, P.-Y. Lesaicherre, T. Sakuma, Y. Miyasaka, A. Ishitani, and M. Yoshida, Jpn. J. Appl. Phys. **32**, 4069 (1993).
[6]P.-Y. Lesaicherre, H. Yamaguchi, T. Sakuma, Y. Miyasaka, M. Yoshida, and A. Ishitani, Mater. Res. Soc. Symp. Proc. **310**, 487 (1993).
[7]T. Kimura, H. Yamauchi, H. Machida, H. Kokubun, and M. Yamada, Jpn. J. Appl. Phys. **33**, 5119 (1994).
[8]S. Liang, C. S. Chern, Z. Q. Shi, P. Lu, A. Safari, Y. Lu, B. H. Kear, and S. Y. Hou, Appl. Phys. Lett. **64**, 3563 (1994).
[9]I. Kobayashi, Y. Wakao, K. Tominaga, and M. Okada, Jpn. J. Appl. Phys. **33**, 4680 (1994).
[10]T. Kawahara, M. Yamamuka, T. Makita, J. Naka, A. Yuuki, N. Mikami, and K. Ono, Jpn. J. Appl. Phys. **33**, 5129 (1994).
[11]J. M. Zhang, F. DiMeo, Jr., B. W. Wessels, D. L. Schulz, T. J. Marks, J. L. Schindler, and C. R. Kannewurf, J. Appl. Phys. **71**, 2769 (1992).
[12]H. Harima, H. Ohnishi, K. Hanaoka, K. Tachibana, M. Kobayashi, and S. Hoshinouchi, Jpn. J. Appl. Phys. **29**, 1932 (1990).